ChemComm

Accepted Manuscript

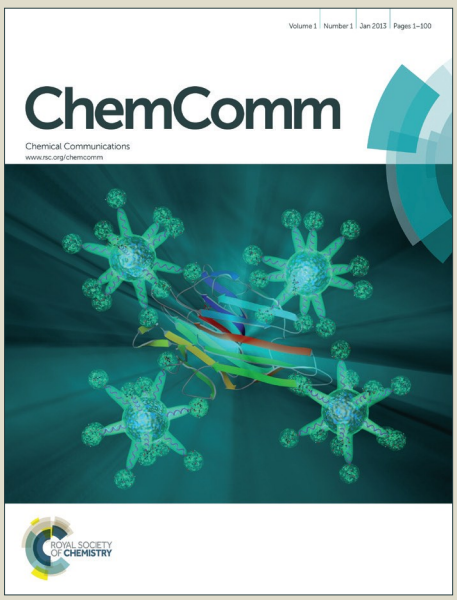

ROYAL SOCIETY OF CHEMISTRY

www.rsc.org/chemcomm

ChemComn

RSCPublishing

COMMUNICATION

Facile Construction of Well-defined Fullerene-Dendrimer Supramolecular Nanocomposites for Bioapplications

Cite this: DOI: 10.1039/xoxxoooooox

Received ooth January 2012,
Accepted ooth January 2012

DOI: 10.1039/xoxxoooooox

www.rsc.org/chemcomn

Xiaojie Li,[a] Yasuo Watanabe,[a] Eiji Yuba,[a] Atsushi Harada,[a] Takeharu Haino [b] and Kenji Kono*[a]

Well-defined fullerene-dendrimer supramolecular nanocomposites exhibiting uniform size, controlled morphology, high fullerene inclusion efficiency, excellent water solubility, and non-toxicity were facilely fabricated through complexation of carboxyfullerenes with poly(ethylene glycol)-modified poly(amidoamine) dendrimers.

Fullerene (C_{60}) and its derivatives, because of their unique nanoscale physical and chemical properties, have attracted particular interest in biomedical applications such as cancer diagnostics and therapy, including magnetic resonance imaging (MRI),[1] drug and gene delivery,[2] photothermal therapy,[3] and photodynamic therapy (PDT).[4,5] Despite their great potential in biomedical science, current small molecular size fullerenes are still not widely used in real applications, probably because of their potential toxicity and limited specificity and efficacy. To address these limitations, many biocompatible polymers have been attached covalently onto fullerene to obtain fullerene-polymer nanocomposites with low toxicity and the aim to accumulate in tumor tissues selectively through enhanced permeability and retention (EPR) effects.[6–8] However, covalent bonds linking polymer and fullerene might alter the electron structure of fullerene and polymers dramatically, resulting in a loss or reduction of the expected functions of fullerene-polymer nanocomposites.[9] As an alternative and promising strategy, fullerene-polymer supramolecular nanocomposites constructed through non-covalent bonds with only slightly distorted electronic structure have exhibited prominent potential in the field of photovoltaics.[9–11] Most reported polymeric hosts for fullerene are water-insoluble. They invariably involve toxic components for the formation of π-π stacking interactions with fullerene,[12–16] therefore rendering them unsuitable for biomedical applications. Moreover, it remains a great challenge to generate fullerene-polymer nanocomposites with high loading density, narrow size distribution, and homogeneous morphology. Further endeavors should be made for clinical applications to develop water-soluble polymeric fullerene supramolecular nanocomposites showing specific targeting, biocompatibility, and controlled morphology.

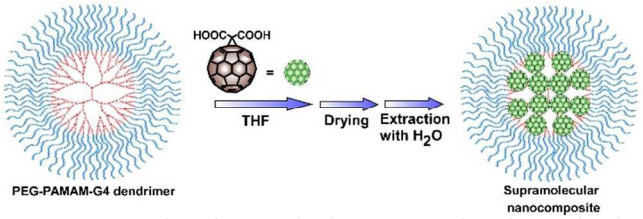

Scheme 1 Preparation of supramolecular nanocomposites via complexation of carboxyfullerenes and PEG-modified PAMAM G4 dendrimer.

Dendrimers are a class of artificial polymers with well-defined composition, branched tree-like structure, and versatile component units for additional functionalization.[17–19] Because of their high coordination properties to metal salts, dendrimers have been used for precise synthesis of various dendrimer-metal nanoparticles and dendrimer-metal oxide subnanoparticle nanocomposites.[19–21] It can be inferred that if the fullerene molecules can coordinate selectively with dendrimers, promising fullerene-dendrimer supramolecular nanocomposites integrating the advantages of fullerenes and those of dendrimers can be expected. This report describes a facile and high-efficiency strategy for the construction of well-defined fullerene-dendrimer supramolecular nanocomposites using poly(ethylene glycol)-modified poly(amidoamine) (PEG-PAMAM) dendrimers and carboxyfullerenes. Because of its nontoxicity, uniform size, thermodynamic stability, and improved pharmacokinetics and biodistribution profiles, PEG-PAMAM dendrimers composed of a biocompatible PEG surface and a commercially available PAMAM dendrimer interior are used as the host for fullerenes.[22,23] Well-established fullerene derivatives, carboxyfullerenes, are used to form supramolecular nanocomposites with PEG-PAMAM dendrimers because of its appropriate molecular structure composed of a hydrophobic fullerene part and negatively charged groups, showing strong affinity to PAMAM dendrimer interior through both hydrophobic interaction and electrostatic interaction.[23] The resulting fullerene-dendrimer supramolecular nanocomposites are expected to promote their accumulation at tumor tissues via the EPR effect and to maintain the fullerenes photophysical activity simultaneously, greatly enhancing their therapeutic efficacy.

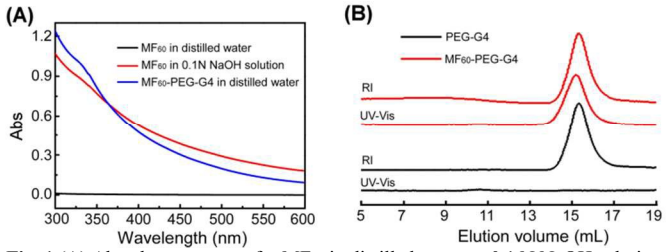

Fig. 1 (A) Absorbance spectra for MF_{60} in distilled water or 0.1 N NaOH solution and MF_{60}-PEG-G4 nanocomposites in distilled water. (B) Aqueous GPC traces of PEG-G4 dendrimer and MF_{60}-PEG-G4 nanocomposites.

The strategy for preparing supramolecular nanocomposites of fully PEG-modified generation 4 PAMAM dendrimers[24] (PEG-G4) and mono-malonic acid C_{60}[25] (MF_{60}) is shown in Scheme 1. Typically, PEG-G4 dendrimers and MF_{60} were dissolved in tetrahydrofuran (THF) and incubated for 1 h, during which the supramolecular nanocomposites of MF_{60} with PEG-G4 dendrimer were formed because of the electrostatic interaction. Then, THF was evaporated under reduced pressure to give a thin film. Actually, MF_{60} is only soluble in basic water (pH > 9), but it is insoluble in distilled water (Fig. 1A). Therefore, the resulting MF_{60}-PEG-G4 nanocomposites were obtained facilely by extraction from the dry film using distilled water. The insoluble precipitate, mostly un-included MF_{60}, was removed by centrifugation. As shown in Fig. 1A, MF_{60}-PEG-G4 in distilled water showed a similar UV–Vis absorption with free MF_{60} in 0.1 N NaOH, indicating that PEG-G4 dendrimers form an inclusion complex with MF_{60} with high efficiency and good water-solubility. Moreover, the MF_{60}-PEG-G4 nanocomposites were characterized using gel permeation chromatography (GPC) analysis. PEG-G4 dendrimer without fullerenes was used as a control. As shown in Fig. 1B, the PEG-G4 dendrimer peak appeared only by refractive index (RI) analysis, but the signal of MF_{60}-PEG-G4 nanocomposites was observed from both RI analysis and UV–Vis (426 nm) analysis at the same elution volume range, indicating that MF_{60} were tightly included within the PEG-G4 dendrimers. No marked volume difference was observed between the empty and MF_{60}-including PEG-G4 dendrimers.

According to our design, both hydrophobic and electrostatic interactions are attributable to the high inclusion efficiency and good stability of MF_{60}-PEG-G4 nanocomposites. To verify this hypothesis, fullerenes of four kinds were used to prepare nanocomposites with PEG-G4 dendrimers at various fullerene/dendrimer feed ratios. The fullerene-PEG-G4 nanocomposites were extracted using distilled water. The numbers of included fullerenes per PEG-G4 dendrimer were quantified from their UV–Vis absorbance in THF. As Fig. 2A shows, no pristine fullerenes and only approx. 4 mono-(diethyl malonate) fullerene molecules were bound into each PEG-G4 dendrimer, independent of feed ratios. The number of MF_{60} and DF_{60} included with each PEG-G4 dendrimer increased with the feed ratios and finally reached a maximum value. Previously, we demonstrated that the electrostatic interaction between inner tertiary amino groups of PAMAM dendrimers and carboxyl groups of guest molecules is a crucial driving force for inclusion complex formation.[26] This report presents the low inclusion complex formation efficiency for pristine fullerenes and mono-malonate fullerenes results from the lack of such driving forces. Regarding carboxyfullerenes, each dendrimer can bind a maximum of 80 MF_{60} and 35 DF_{60} molecules, respectively, with 80 and 70 malonic acid groups. Considering that each G4 PAMAM dendrimer has only 62 tertiary amine groups, their complexation might not be induced simply through their electrostatic interaction; their hydrophobic interaction might also contribute to their complex formation.

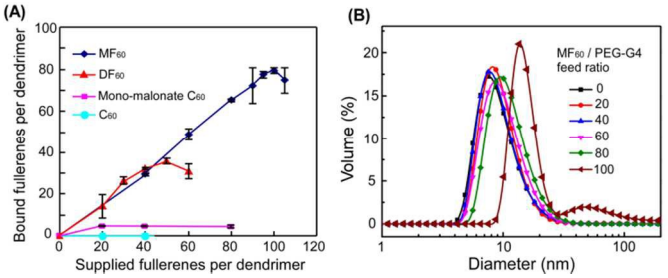

Fig. 2 (A) Supramolecular nanocomposites formation of four kinds of fullerenes with PEG-G4 dendrimer at varying fullerene/dendrimer feed ratios. (B) Size distribution of MF_{60}-PEG-G4 nanocomposites prepared at various fullerene/dendrimer feed ratios. DF_{60} and C_{60} denote di-malonic acid C_{60} and unmodified pristine fullerene C_{60}, respectively.

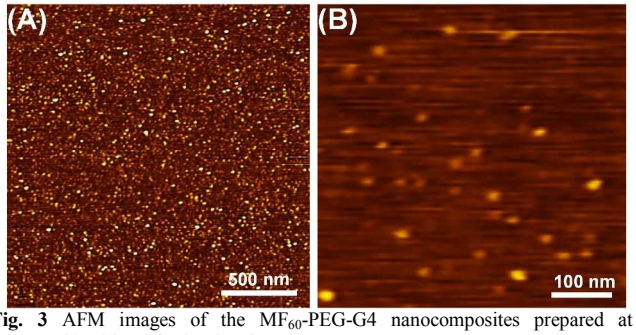

Fig. 3 AFM images of the MF_{60}-PEG-G4 nanocomposites prepared at a fullerene/dendrimer feed ratio of 80.

To confirm that MF_{60} were included within the dendrimer moiety, the ^1H NMR spectrum of MF_{60}-PEG-G4 in D_2O was measured and compared with that of empty PEG-G4 (Fig. S1, ESI†). Both PEG and PAMAM dendrimer signals were observed in empty PEG-G4, but only PEG signals were observed in MF_{60}-PEG-G4. The complete disappearance of the PAMAM dendrimer signals in MF_{60}-PEG-G4 indicates that hydrophobic MF_{60} molecules were truly held in the PAMAM dendrimer moiety of the MF_{60}-PEG-G4 nanocomposite. Furthermore, oligo(ethylene glycol)-modified generation 4 PAMAM dendrimer (OEG-G4) with a shorter surface PEG chain length than PEG-G4 was used to prepare nanocomposites with MF_{60} at a fullerene/dendrimer feed ratio of 40. The MF_{60} inclusion efficiencies for PEG-G4 and OEG-G4 were, respectively, 81.3% and 70.0%, indicating that about 33 and 28 MF_{60} molecules were encapsulated in the PEG-G4 and OEG-G4, respectively (Fig. S2, ESI†). Considering that OEG chains are too short to stabilize the MF_{60} molecules, all the included MF_{60} should be within the dendrimer interior. The 11.3% higher of inclusion efficiency for PEG-G4 than OEG-G4 is probably attributable to the benefit of long hydrophilic PEG chains which cover the MF_{60} molecules bound to the dendrimer interior efficiently and increase their colloidal stability. These results are also supported by the fact that PEG-modified generation 5 PAMAM dendrimer (PEG-G5) with a larger dendrimer interior than PEG-G4 can include a maximum of 97.5 MF_{60} molecules per dendrimer, indicating a greater capability of PEG-G5 to encapsulate MF_{60} molecules (Fig. S3, ESI†).

The detailed structures of MF_{60}-PEG-G4 nanocomposites were further elucidated by dynamic light scattering (DLS) and atomic force microscopy (AFM) analysis. The nanocomposites were prepared at varying fullerene/dendrimer feed ratios. As shown in Fig. 2B, the average diameters of PEG-G4 were determined to be 9.5 nm by mass. The diameters of MF_{60}-PEG-G4 nanocomposites increased gradually to 11.6 nm in the fullerene/dendrimer feed range of 20–80. However, the particle size of MF_{60}-PEG-G4 nanocomposites increased dramatically at the fullerene/dendrimer feed ratio of 100.

Reportedly, the PEG chains of PEG-PAMAM dendrimers can penetrate into the PAMAM dendrimer moiety in aqueous solutions.[27] Therefore, the initially slight increase in hydrodynamic diameter of MF_{60}-PEG-G4 compared to PEG-G4 might result from extended PEG chains after MF_{60} loading into the PAMAM dendrimer interior. Moreover, the inclusion of MF_{60} into PAMAM dendrimer moiety might induce the size increase of dendrimer interior. When the fullerene/dendrimer feed ratio increased to 100, the resulting MF_{60}-PEG-G4 might contain too much MF_{60} molecules with hydrophobic character and start to aggregate to larger nanoparticles and then precipitate. AFM images for MF_{60}-PEG-G4 nanocomposites prepared at a fullerene/dendrimer feed ratio of 80 showed discrete spherical particles without aggregation at both high concentration (Fig. 3A) and low concentration (Fig. 3B). And no obvious morphology change was observed compared with PEG-PAMAM-G4 dendrimer alone (Fig. S4, ESI†). Cross-sectional analysis showed that the average diameter of the MF_{60}-PEG-G4 nanocomposites in AFM images was ~ 10.2 nm. Considering the shrinkage effect in the dry state during AFM sample preparation, this value agrees well with the DLS result, thereby indicating the stable and uniform 'supramolecular core–shell' structure of obtained MF_{60}-PEG-G4 nanocomposites with a PEG shell and a MF_{60}-PAMAM nanocomposite core.

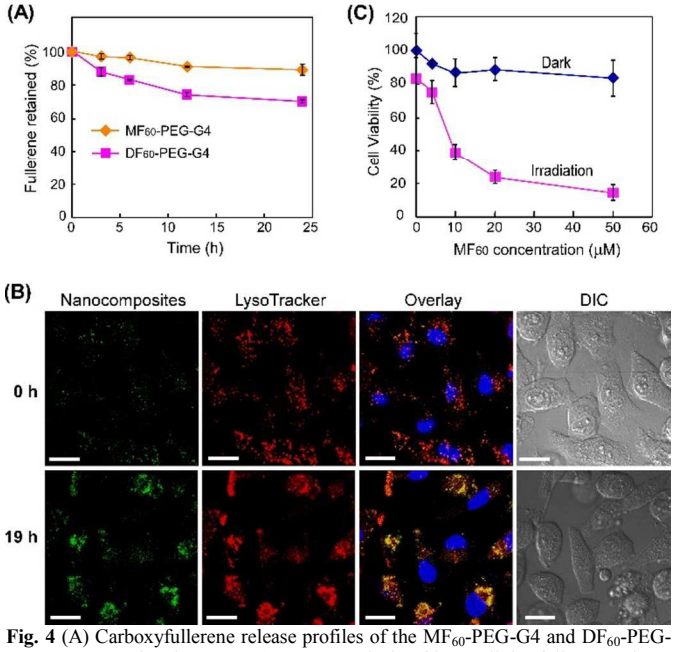

Fig. 4 (A) Carboxyfullerene release profiles of the MF_{60}-PEG-G4 and DF_{60}-PEG-G4 nanocomposites in PBS. (B) CLSM analysis of intracellular fullerene release from MF_{60}-FI-PEG-G4 nanocomposites. HeLa cells were treated with MF_{60}-FI-PEG-G4 nanocomposites for 5 h and washed, followed by CLSM observation after 0 or 19 h. Nucleus was stained with Hoechst 33342. Scale bar represents 20 μm. (C) Cytotoxicity of the MF_{60}-PEG-G4 nanocomposites against HeLa cells in the dark or under laser irradiation.

The PEG-PAMAM dendrimer-based drug delivery systems often suffer from the problem of a quick release of their encapsulated therapeutic agents,[24,26] which limits their biomedical applications. The release behaviour of carboxyfullerenes (MF_{60} and DF_{60}) from their nanocomposites with PEG-G4 was investigated using dialysis in pH 7.4 PBS. The residual carboxyfullerenes were measured using UV–Vis absorbance. As shown in Fig. 4A, ~ 10% MF_{60} and ~ 30% DF_{60} were released after 24 h incubation in PBS, meaning that DF_{60} containing two hydrophilic malonic acid groups was released more rapidly than MF_{60} containing only one malonic acid. As described above, the inclusion complex formation of nanocomposites depends on the electrostatic interaction. However, the electrostatic interaction is suppressed under isotonic conditions in PBS. Therefore, the hydrophobicity of carboxyfullerenes might dominate the stability of nanocomposites. FITC-labelled PEG-G4 dendrimers (FI-PEG-G4) was synthesized and used to prepare nanocomposites. The resulting MF_{60}-FI-PEG-G4 nanocomposites were used for cell internalization and intracellular release study. Fluorescence of FI-PEG-G4 was markedly quenched by inclusion of fullerenes after formation of MF_{60}-FI-PEG-G4 nanocomposites (Fig. S5). Therefore, the recovery of fluorescence was used for detection of MF_{60} release from MF_{60}-FI-PEG-G4 nanocomposites. HeLa cells were treated with MF_{60}-FI-PEG-G4 nanocomposites for 5 h, and then washed with PBS. The cells were observed with confocal laser scanning microscopy (CLSM) just after washing or after another 19 h-incubation in the culture medium (Fig. 4B). A weak green fluorescence derived from MF_{60}-FI-PEG-G4 nanocomposites was observed just after 5 h incubation, which suggests that MF_{60} molecules were hardly released from the composites in such a short time. However, after another 19 h incubation, intensity of green fluorescence became stronger, indicating the recovery of the dendrimer fluorescence. Nearly all lysosomes, which displayed red fluorescence, included green fluorescence dots in the overlay images, suggesting that MF_{60}-FI-PEG-G4 nanocomposites were trafficked into lysosomes, and then MF_{60} molecules were gradually released inside of lysosomes. These results indicate that MF_{60}-PEG-G4 nanocomposites can keep the carboxyfullerene molecules stably at physiological pH and release them in lysosomes with an acidic pH environment. To investigate the potential PDT performance of MF_{60}-PEG-G4 nanocomposites against cancer cells, an *in vitro* viability assay against HeLa cells was then performed. As shown in Fig. 4C, MF_{60}-PEG-G4 in dark exhibited negligible cytotoxicity towards Hela cells. However, HeLa cells treated with MF_{60}-PEG-G4 nanocomposites and 3 h light irradiation showed prominent cytotoxicity in a dosage-dependent manner, indicating the controllable and selective photodynamic cytotoxic effects of nanocomposites.

In summary, we developed a facile and high-efficiency strategy for the construction of well-defined fullerene-dendrimer supramolecular nanocomposites using PEG-PAMAM dendrimers as the host for carboxyfullerenes. The supramolecular nanocomposites exhibit excellent water solubility and colloidal stability in biological environments. Moreover, this report describes the first monodispersed fullerene-polymer supramolecular nanocomposites with a uniform morphology and high fullerene loading efficiency, integrating both the structural advantages of dendrimers and the photoactivable properties of fullerenes. Considering that both dendrimer and fullerene are versatile nanoplatforms for various functions, well-defined fullerene-dendrimer supramolecular nanocomposites are expected to find widespread application in various fields of nanobiotechnology.

Notes and references

[a] Department of Applied Chemistry, Graduate School of Engineering, Osaka Prefecture University, 1-1 Gakuen-cho, Naka-ku, Sakai, Osaka 599-8531, Japan. E-mail: kono@chem.osakafu-u.ac.jp; Fax: +81-072-254-9330; Tel: +81-072-254-9330
[b] Department of Chemistry, Graduate School of Science, Hiroshima University, 1-3-1 Kagamiyama, Higashi-Hiroshima City 739-8526, Japan.
† Electronic Supplementary Information (ESI) available: Detailed synthesis and characterization of dendrimers and fullerene derivatives, and their nanocomposites formation. See DOI: 10.1039/c000000x/

1 Z. Y. Chen, L. J. Ma, Y. Liu and C. Y. Chen, *Theranostics*, 2012, **2**, 238-250.
2 A. Montellano, T. Da Ros, A. Bianco and M. Prato, *Nanoscale*, 2011, **3**, 4035-4041.

3 V. Krishna, A. Singh, P. Sharma, N. Iwakuma, Q. Wang, Q. Zhang, J. Knapik, H. Jiang, S. R. Grobmyer, B. Koopman and B. Moudgil, *Small*, 2010, **6**, 2236-2241.
4 P. Mroz, G. P. Tegos, H. Gali, T. Wharton, T. Sarna and M. R. Hamblin, *Photochem. Photobiol. Sci.*, 2007, **6**, 1139-1149.
5 S. K. Sharma, L. Y. Chiang and M. R. Hamblin, *Nanomedicine*, 2011, **6**, 1813-1825.
6 Y. Tabata, Y. Murakami and Y. Ikada, *Jpn. J. Cancer Res.*, 1997, **88**, 1108-1116.
7 J. Liu, S.-i. Ohta, A. Sonoda, M. Yamada, M. Yamamoto, N. Nitta, K. Murata and Y. Tabata, *J. Controlled Release*, 2007, **117**, 104-110.
8 Y. Iwamoto and Y. Yamakoshi, *Chem. Commun.*, 2006, 4805-4807.
9 E. Badamshina and M. Gafurova, *Journal of Materials Chemistry*, 2012, **22**, 9427-9438.
10 F. Giacalone and N. Martín, *Advanced Materials*, 2010, **22**, 4220-4248.
11 S. S. Babu, H. Mohwald and T. Nakanishi, *Chem. Soc. Rev.*, 2010, **39**, 4021-4035.
12 W. Li, X. Zhu, J. Wang, R. Liang, J. Li, S. Liu, G. Tu and J. Zhu, *J. Colloid Interface Sci.*, 2014, **418**, 81-86.
13 M. C. Stuparu, *Angew. Chem., Int. Ed.*, 2013, **52**, 7786-7790.
14 X.-S. Wang, T. Metanawin, X.-Y. Zheng, P.-Y. Wang, M. Ali and D. Vernon, *Langmuir*, 2008, **24**, 9230-9232.
15 X.-H. Dong, W.-B. Zhang, Y. Li, M. Huang, S. Zhang, R. P. Quirk and S. Z. D. Cheng, *Polym. Chem.*, 2012, **3**, 124-134.
16 N. Fujita, T. Yamashita, M. Asai and S. Shinkai, *Angew. Chem., Int. Ed.*, 2005, **44**, 1257-1261.
17 D. Astruc, E. Boisselier and C. Ornelas, *Chem. Rev.*, 2010, **110**, 1857-1959.
18 S. M. Grayson and J. M. J. Fréchet, *Chem. Rev.*, 2001, **101**, 3819-3868.
19 D. A. Tomalia, *Soft Matter*, 2010, **6**, 456-474.
20 K. Yamamoto and T. Imaoka, *Acc. Chem. Res.*, 2014, **47**, 1127-1136.
21 L. M. Bronstein and Z. B. Shifrina, *Chem. Rev.*, 2011, **111**, 5301-5344.
22 Y. Cheng, L. Zhao, Y. Li and T. Xu, *Chem. Soc. Rev.*, 2011, **40**, 2673-2703.
23 K. Kono, *Polym. J.*, 2012, **44**, 531-540.
24 C. Kojima, K. Kono, K. Maruyama and T. Takagishi, *Bioconjugate Chem.*, 2000, **11**, 910-917.
25 L. L. Dugan, D. M. Turetsky, C. Du, D. Lobner, M. Wheeler, C. R. Almli, C. K.-F. Shen, T.-Y. Luh, D. W. Choi and T.-S. Lin, *Proc. Natl. Acad. Sci. U. S. A.*, 1997, **94**, 9434-9439.
26 C. Kojima, Y. Toi, A. Harada and K. Kono, *Bioconjugate Chem.*, 2007, **18**, 663-670.
27 H. Lee and R. G. Larson, *Macromolecules*, 2011, **44**, 2291-2298.

TOC